AIJREAS VOLUME 1, ISSUE 7 (2016, JULY) (ISSN-2455-6300) ONLINE
ANVESHANA'S INTERNATIONAL JOURNAL OF RESEARCH IN ENGINEERING AND APPLIED SCIENCES

IDENTIFICATION OF SEA-ICE FLOES AND FLOE SIZE DISTRIBUTIONS USING IMAGE PROCESSING

P.GANGADHARA REDDY[1], M. RENUKA[2], R.SAI NAVEENA[3] , C.B.ROHINI[4]

[1]Assistant professor in ECE, ADITYA COLLEGE OF ENGINEERING Madanapalle, A.P., INDIA
[2, 3, 4] Students, Dept. of ECE, ADITYA COLLEGE OF ENGINEERING Madanapalle, A.P.,INDIA
E-Mail: gangadhararedd y.p@gmail.com[1]
renu20547@gmail.com[2]

ABSTRACT:
An unmanned aerial vehicle was used as a mobile sensor platform to collect sea-ice features at Ny-Ålesund in early May 2011, and several image processing algorithms have been applied to samples of sea-ice images to extract useful information about sea ice. The sea-ice statistics given by the floe size distribution, being an important parameter for climate and wave- and structure-ice analysis, is challenging to calculate due to difficulties in ice floe identification; particularly snake algorithm is applied to solve this problem. To evolve the GVF snake algorithm automatically, an initialization based on the distance transform is proposed to detect individual ice floes, and the morphological cleaning is afterward applied to smoothen the shape of each identified ice floe. Based on the identification result, the image is separated into four different layers: ***ice floes, brash pieces, slush, and water****.. The proposed algorithm implements Otsu Thresholding method, K-Means clustering algorithm, Distance transform, edge detection and morphology operation yields an acceptable identification result. A discussion on the methods and results concludes the paper.*

Index Terms: *Floe size distribution, ice floe identification, image processing, marginal ice zone, remote sensing.*

1. INTRODUCTION:

SEA ICE, which is defined as any form of ice that forms as a result of seawater freezing [2], covers approximately 7% of the total area of the world's oceans [3]. It is turbulent because of wind, wave, and temperature fluctuations. Various types of sea ice can be found in ice-covered regions. Ice floe, which is the flat pieces of sea ice, can range from meters to kilometers in size. The floe size distribution is a basic parameter of sea ice that affects the behavior of sea-ice extent, both dynamically and thermodynamically. Particularly for relatively small ice floes, it is critical to the estimation of melting rate [4]. Hence, estimating floe size distributions contributes to the understanding of the behavior of the sea-ice extent on a global scale. In addition to this, the floe size distribution is also important in ice management for Arctic offshore operations [5], [6], for example:

• Quantify the efficiency of ice management for Arctic offshore operations and automatically detect hazardous conditions, for example, by identifying large floes that escape the icebreakers operating upstream of a protected structure. The size and shape of managed floes can be identified by the image processing system, compared with limit values, and further processed by the risk management system.
• Provide an early warning of an ice compaction event, which can be dangerous if the ice-structure interaction mode changes from a "slurry flow" type to a "pressured ice" type [8], [15].

Therefore, the development of temporally and spatially continuous field observations of sea-ice conditions and determining corresponding ice floe size distributions are necessary.

One of the best ways to observe ice conditions in the oceans is by using aerial imagery and applying digital image processing techniques to the observations. This method can reduce or suppress ambiguities, incompleteness, uncertainties, and errors regarding an object and its environment, yielding more accurate and reliable information [16]. Cameras are typically used as sensors on mobile sensor platforms in ice-covered regions to characterize ice conditions [17], [18]. Cameras can collect precise spatially continuous measurements, which are particularly suitable for providing detailed localized information of sea ice. However, an important prerequisite is a clear sky and sight during missions.

A remote sensing mission to determine ice conditions was performed by the Northern Research Institute (NORUT) at 78◦55_ N 11◦56_ E, Hamnerabben, Ny-Ålesund, from May 6 to 8, 2011. An unmanned aerial vehicle (UAV) was used as a mobile sensor platform because of its flexibility in coverage and in spatial and temporal resolution, which are three important sensor-

platform attributes. The use of cameras as sensors on a UAV was explored to measure ice statistics and properties.

Fig. 1.1. CryoWing UAV operation at Ny-Ålesund (photographer: Qin Zhang).

Objective of the mission was to gather information about the ice conditions in the Arctic. The further goal was to develop tools based on the processed ice data that can be applied for decision support in Arctic offshore operations. A Cryo Wing [19] UAV, as shown in Fig. 1.1, was used for the mission. This UAV was designed for cryospheric measurements and environmental monitoring,. The basic instrumentation of the CryoWingis an onboard computer that controls the different payload instruments, stores data to a solid-state disk, and relays data to the ground. The onboard payload system has a GPS receiver and a three-axis orientation sensor that is independent of the avionics system. The sensor device used in this analysis is a digital visual camera.

The UAV flew in the inner part of Kongsfjorden to collect high-resolution images of sea ice. Several image-processing algorithms have then been applied to these images to extract useful information of the sea ice, such as ice concentration, ice floe boundaries, and ice types [18].Automatic identification of individual floe edges is a key tool for extracting information of floe size distribution from aerial images. In an actual ice-covered environment, ice floes typically touch each other, and the junctions may be difficult to identify in digital images. This issue challenges the boundary detection of individual ice floes and significantly affects ice floe size analysis. Several researchers have tried to mitigate this issue. In [20] and [21], the authors separated closely distributed ice floes by setting a threshold higher than the ice-water segmentation threshold and separated the connected ice floes manually when the threshold did not work well. In [18] and [22], the authors applied and compared derivative and morphology boundary detection algorithms in both model ice and sea-ice images. However, non closed boundaries are often produced by traditional derivative boundary detection, while some boundary information is often lost by morphology boundary detection. To separate connected sea-ice floes into individual floes, the watershed transform (widely used in connected object segmentation) was adopted in [23] and [24]. Due to an ineluctable over segmentation problem of the watershed-based method, the authors in [23] manually removed these over segmented lines, while those in [24] automatically removed the over segmented lines whose endpoints were both convex. However, over- and under segmentation still affected the ice floe detection results. In [25] and [26], the authors introduced a mathematical morphology together with principal curve clustering to identify ice floes and their boundaries in an almost fully automated manner.

To separate seemingly connected floes into individual ones, a gradient vector flow (GVF) snake algorithm [27] is applied in this research. However, to start the algorithm, a proper initial contour is required for the GVF snake to evolve correctly. Therefore, a manual initialization is typically needed, particularly in crowded floe segmentation. To solve this problem, an automatic contour initialization is proposed to avoid manual interaction and reduce the time required to run the algorithm. Once individual ice floes have been identified, the floe boundaries are obtained, and the floe size distribution can be calculated from the resulting data.

Image processing is a technique to enhance raw images received from cameras/sensors placed on satellite, space probes and aircraft or pictures taken in normal day-to-day life for various applications.

Various techniques have been developed in image processing during the last four to five decades. Most of the techniques are developed for enhancing images obtained from unmanned spacecrafts, space probes and military reconnaissance flights. Image processing systems are becoming popular due to easy availability of

powerful personnel computers, large size memory devices, graphics software's etc..,

2. ICE IMAGE PROCESSING METHODS:

2.1 IMAGE:

An image is represented as a 2-d function f(x,y) where x and y are spatial co-ordinates and amplitude of 'f' at any pair of coordinates(x,y) is called the intensity of the image at that point.

2.2 TYPES OF IMAGES:

The toolbox supports four types of images:
1. Intensity images
2. Binary images
3. Indexed images
4. RGB images

Most monochrome image processing operations are carried out using binary or intensity images, so our initial focus is on these two image types Indexed and RGB color

2.3 ICE IMAGE PROCESSING METHODS:

- Ice pixel extraction
- Ice edge detection
- Ice shape enhancement
- Ice type classification and Floe size distribution

2.3.1 ICE PIXEL EXTRACTION:

Ice pixels have higher intensity values than those belonging to water in a uniform illumination ice image. Ice pixels can be extracted by using two methods they are Thresholding method and k-means algorithm.

2.3.1.1 THRESHOLDING METHOD: The pixels in the same region have similar intensity, and thresholding is a natural way to segment such regions. It is based on the pixel's gray-level to turn a grayscale image into a binary image. The threshold value is chosen to separate an image into an "object region" and a "background region". For a grayscale image, assuming that an object is brighter than the background, the object and background pixels have intensity levels grouped into two dominant modes. The threshold T is selected to extract the objects from the background. Individual pixels are marked as "object" pixels if their value is greater than the threshold value and as "background" pixels otherwise, that is,

$$g(x,y) = \begin{cases} 1 & if\ f(x,y) \geq T \\ 0 & if\ f(x,y) < T, \end{cases}$$

Where T is the threshold value, and g(x , y) and f(x , y) are the pixel values located in the thx column, thy row of the binary and grayscale image, respectively.

The key of this method is how to select the threshold value, for which there are several different methods. When a constant threshold value is used over the image, it is called global thresholding. Otherwise, it is called local thresholding, which allows the threshold value to vary over the image.

2.3.1.1.1 OTSU THRESHOLDING:

The Otsu thresholding method is one of the most common global threshold segmentation algorithms. It is used to perform histogram shape-based image thresholding automatically. The assumptions of the Otsu thresholding method are:

• The illumination is uniform.

The histogram is divided into two classes (i.e., the pixels are identified as either foreground or background), and the goal is to find the threshold value that minimizes the within-class variance, given by:

$$\sigma_{\varphi}^2(T) = \omega_1(T)\sigma_1^2(T) + \omega_2(T)\sigma_2^2(T),$$

where 1ω, 2ω are the probabilities of the two classes separated by a threshold T and, σ_1^2, σ_2^2 are the variances of these two classes. The threshold with the maximum between-class variance also has the minimum within-class variance. According to, the between-class variance is given by:

$$\sigma_b^2 = \omega_1(T)[\mu_1(T) - \mu(T)]^2 + \omega_2(T)[\mu_2(T) - \mu(T)]^2$$

$$\cong \omega_1(T)\omega_2(T)[\mu_1(T) - \mu_2(T)]^2$$

Where μ_1, μ_2 are the means of these two classes, and $\mu(T) = \omega_1(T)\mu_1(T) + \omega_2(T)\mu_2(T)$

2.3.2 ICE EDGE DETECTION :

The floe size distribution is a basic parameter of sea-ice that affects the behavior of sea-ice extent both dynamically and thermodynamically. It is also important in ice management for Arctic offshore

operations. Automatic identification of individual floe boundaries is a key tool for extracting information of floe size distribution from sea-ice images. In an actual ice-covered environment, ice floes typically touch each other, and the junctions may be difficult to identify in digital images. This issue challenges the boundary detection of individual ice floes, and it significantly affects ice floe size analysis.

Several methods, such as derivative boundary detection, morphology-based method, watershed based Algorithms, have been applied to identify the floe boundaries. However, those methods are limited when trying to identify a boundary that is hidden. Zhang and Skjetne introduce the Gradient Vector Flow (GVF) Snake algorithm, which has a good detection capability of weak boundaries. Together with the distance transform, this is used to identify ice floes and their boundaries automatically.

2.3.3 ICE SHAPE ENHANCEMENT:

Because of the noise, some floes may contain holes or smaller ice pieces inside shows an ice floe with speckle. Because of the uneven gray scale of the ice floe, the lighter part .of the floe is considered as "light ice" [the white pixels in segmentation result and shape enhancement result], whereas the darker part is considered as "dark ice" [the gray pixels]by the k-means and threshold method. This means that the ice floe cannot be completely identified, and the shape of the detected ice floe is rough.

To smoothen the shape of the ice floe, morphological cleaning is used after ice floe identification. Morphological cleaning is a combination of first morphological closing and then morphological opening on an image. Morphological closing tends to smooth the contours of objects, generally joins narrow breaks, fills long thin gulfs, and fills holes smaller than the structuring element, while morphological opening removes complete regions of an object that cannot contain the structuring element, smooth's object contours, breaks thin connections, and removes thin protrusions. Using this method, all the "light ice" and "dark ice" pieces in the sea-ice segmentation image are first arranged from small to large. Then, morphological cleaning with disk-shaped structuring element is performed to the arranged ice pieces in sequence, and the radius of disk-shaped structuring element is adapted to the size of each ice piece automatically. This process will ensure the completeness of the ice floe, and smaller ice floes or brash pieces contained in a lager ice floe are removed. The shape enhancement result. After shape enhancement, collecting and labeling all the cleaned ice pieces. To present a better visualization of the sizes (defined as the pixel number of each ice piece), the ice pieces are labeled in different colors based on the formula.

$$\text{Color}(p) = \begin{cases} 0, & \text{if } p \notin ICE \\ \left(1 - \exp\left(-\frac{size(i)}{1000}\right)\right) \cdot 10000, & \text{if } p \in ice(i) \end{cases}$$

where p is the pixel, ICE = {ice(1), ice(2), ice(3), . . .} is a set of identified ice pieces, ice(i) ∈ ICE, and size(i) is the pixel number of ice(i). Smaller ice pieces are blue, and larger ice pieces are red. Ice positions, found by averaging the positions of the pixels of each ice piece, are denoted using black dots.

2.3.4 ICE TYPE CLASSIFICATION AND FLOE SIZE DISTRIBUTION:

Brash ice is considered as floating ice fragments no more than 2 m across. To distinguish brash ice from ice floes in our algorithm, we define a brash-ice threshold parameter (pixel number or area) that can be tuned for each application. The ice pieces with size larger than the threshold are considered to be ice floes, while smaller pieces are considered to be brash ice. The remaining ice pixels were is labeled as slush. The result is four layers of a sea-ice image: ice floe brash ice, slush, and water. Based on the four layers, a total of 154 ice floes and 189 brash ice pieces are identified.

The coverage percentage is 60.52% ice floe, 3.34% brash ice, 16.03% slush, and 20.11% water. The ice floe (brash) size can be determined by the number of pixels in the identified floe (brash). If the focal length f and camera height are available, the actual size in SI unit of the ice floes and floe size distribution can be also calculated by converting the image pixel size to its SI unit size. The ice floe size (calculated by counting the pixel number of the floe) distribution histogram. The residue ice, which is the detected boundary pixels between the connected floes, was previously considered as slush(since there often is a boundary layer of slush ice between two ice floes) and

included. However, the residue ice can be also handled specifically according to the applied subsequent processing by the user.

3. IMPLEMENTATION:

3.1 GVF Snake Algorithm:

To evolve the GVF Snake correctly for ice floe boundary detection, a proper initial contour is required. Hang and Skjetne showed that the initial contour close to the actual floe boundary, located inside the floe and centered as close to the ice floe center is most effective. To accomplish the requirements of the initial contour without manual interaction, an automatic contour initialization algorithm based on the distance transform and its local maxima is proposed. This is concluded as:

- **Step 1:** Convert the ice image into binary image after separating the ice from the water, in which case the pixels with value `1' indicate ice and pixels with value`0'indicates water.
- **Step 2:** Perform the distance transform to the binary image. Find the local maxima shown as the green numerals.
- **Step 3:** Merge those local maxima within a short distance by using a dilation operator (Gonzalez et al., 2003). Find the `seeds' that are centers of the dilated regions, shown as red `+' in Figure 4(b) and Figure.
- **Step 4:** Initialize the contours to be located at the seeds with the circular shape. The radius of the circle is then chosen according to the pixel value at the seed in the distance map; see the blue circles.

The circular shape is chosen as the shape of the initial contour, since this shape deforms to the floe boundary more uniformly than other shapes, being unaware of the floes irregular shape and orientation. These methods ensure that the initial contours are located inside the floe and adapted to the floe size. After initializing the contours, the GVF Snake algorithm is run on each contour to identify the floe boundary. Super imposing all the boundaries over the binarized ice image results in separation of the connected ice floes.

3.1.1 INITIAL COUNTER AT DIFFERENT POSITIONS

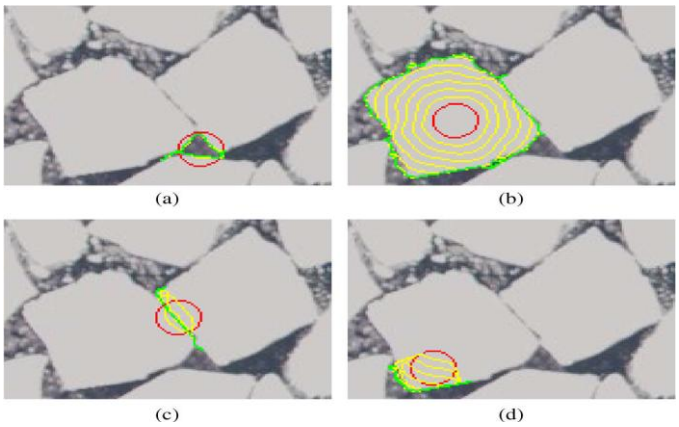

(a)Initial contour 1 located at the water, and the water region boundary is found.

(b) Initial contour 2 located at the center of an ice floe, and the whole floe boundary is found.

(c) Initial contour 3 located at a weak connection, and the weak connection is found

(d) Initial contour 4 located near the floe boundary inside the floe, and only a part of floe boundary is found.

Initial contours located at different positions and their corresponding curve evolutions. The red curves are the initial contours, the yellow curves are iterative runs of the GVF snake algorithm, and the green curves are the final detected boundaries as shown in above figure.

3.2 MORPHOLOGY OPERATION

3.2.1 Mathematical Morphology

The field of mathematical morphology contributes a wide range of operators to image processing, all based around a few simple mathematical concepts from set theory. The operators are particularly useful for the analysis of binary images and common usages include edge detection, noise removal, image enhancement and image segmentation.

The two most basic operations in mathematical morphology are erosion and dilation. Both of these operators take two pieces of data as input: an image to be eroded or dilated, and a structuring element (also known as a kernel). The

two pieces of input data are each treated as representing sets of coordinates in a way that is slightly different for binary and grayscale images.

For a binary image, white pixels are normally taken to represent foreground regions, while black pixels denote background. (Note that in some implementations this convention is reversed, and so it is very important to set up input images with the correct polarity for the implementation being used).

For a grayscale image, the intensity value is taken to represent height above a base plane, so that the grayscale image represents a surface in three-dimensional Euclidean space. Then the set of coordinates associated with this image surface is simply the set of three-dimensional Euclidean coordinates of all the points within this surface and also all points below the surface, down to the base plane. Note that even when we are only considering points with integer coordinates, this is a lot of points, so usually algorithms are employed that do not need to consider all the points.

The structuring element is already just a set of point coordinates (although it is often represented as a binary image). It differs from the input image coordinate set in that it is normally much smaller, and its coordinate origin is often not in a corner, so that some coordinate elements will have negative values. Note that in many implementations of morphological operators, the structuring element is assumed to be a particular shape (e.g. a 3×3 square) and so is hardwired into the algorithm.

Erosion and dilation work (at least conceptually) by translating the structuring element to various points in the input image, and examining the intersection between the translated kernel coordinates and the input image coordinates. To smoothen the rough edges using morphology operation by using MATLAB.

4. RESULTS:

4.1 THRESHOLD METHOD: To extract a light ice from a given sample image by thresholding method is shown below

Fig 4.1.1 Input sample Image

Fig 4.1.2 Light Ice from Thresholding Method

4.2 K-MEANS CLUSTERING:
To extract the dark ice by dividing the image into clusters as shown below

Fig 4.2.1 Input Image

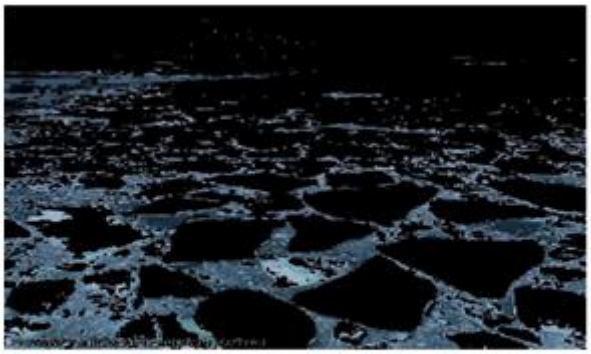

Fig 4.2.2 Dark Ice of object1 from clustering method

Fig 4.2.3 Dark Ice of Cluster2

Fig 4.2.4 Dark Ice from Cluster 3

4.3. DISTANCE TRANSFORM

To obtain the distance between the two ice pieces using distance transform is shown below

Fig 4.3.1 Input Sample Image

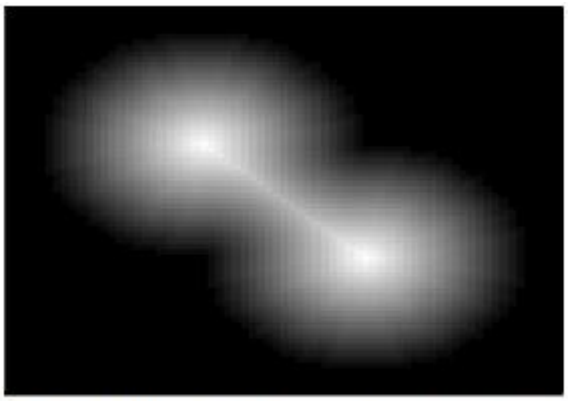

Fig 4.3.2Distance between two ice pieces from Distance Transform

4.4.The identified image is divided into 4 layers of sea ice

1. Ice floe

2. Brash pieces

3. Slush

4 .Water

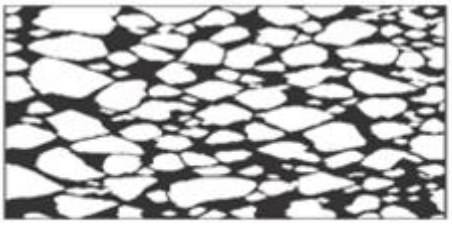

Fig.4.4.1.Layers showing the Ice floe

Fig 4.4.2 Layers showing Brash Ice

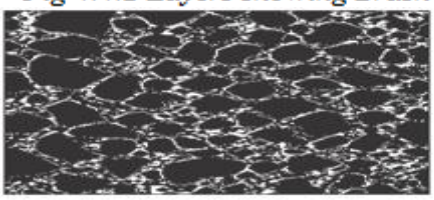

Fig.4.4.3.Layers showing the Slush

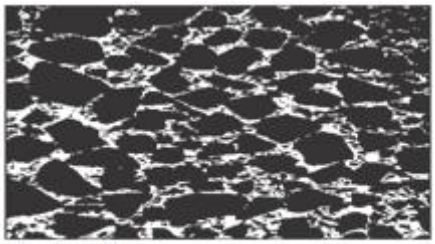

Fig4.4.4 Layers showing the water

5. CONCLUSION

A remote sensing mission yielded experience in data acqui-sition using a UAV. Various image processing methods were applied to a few samples of the collected sea-ice image data for analysis to retrieve important sea-ice information.

Focusing on identifying the non ridged ice floe in the marginal ice zone, and the managed ice resulting from offshore operations in sea ice, we proposed an algorithm to identify the individual ice floes in a sea-ice image using the GVF snake algorithm. To evolve the GVF snake automatically, "light ice" and "dark ice" were first obtained using the thresholding and *k*-means algorithms. The initial contours of both "light ice" and "dark ice" with proper locations and radii were then derived based on the local maxima from the distance transform. After ice edge detection, morphological cleaning was used to enhance floe shapes. The implementation on the sea-ice images, whichcontained multiple ice floes crowded together, is shown to give acceptable segmentation results.

REFERENCES:

[1]. Qin Zhang and Roger Skjetne, "Image processing for Identification of sea ice-floes and the floe size distributions" IEEE Transactions On Geoscience And Remote Sensing, Vol. 53, No. 5, May 2015

[2] S. Løset, K. N. Shkhinek, O. T. Gudmestad, and K. V. Hyland, *Actions from Ice on Arctic Offshore and Coastal Structures*. St. Petersburg, Russia: Lan Publishing House, 2006.

[3] W. Peter, *Ice in the Ocean*. New York, NY, USA: Taylor & Francis,2000.

[4] T. Toyota and H. Enomoto, "Analysis of sea ice floes in the sea of Okhotsk using ADEOS/AVNIR images," in *Proc. 16th IAHR Int. Symp.Ice*, Dunedin, New Zealand, 2002, pp. 211–217.

[5] A. Keinonen, "Ice management for ice offshore operations," in *Proc.Offshore Technol. Conf.*, Houston, TX, USA, 2008, pp. 690–704.

[6] J. Hamilton *et al.*, "Ice management for support of arctic floating operations," in *Proc. OTC Arctic Technol. Conf,*, Houston, TX, USA, 2011,pp. 615–626.

[7] A. Keinonen and I. Robbins, "Icebreaker characteristics synthesis,icebreaker performance models, seakeeping, icebreaker escort," in *Icebreaker*
Escort Model User's Guide: Report Prepared for Transport Development Centre Canada (TP12812E), vol. 3. Calgary, AB, Canada:AKAC, 1998, p. 49.

[8] A. Palmer and K. Croasdale, *Arctic Offshore Engineering*. Singapore: World Scientific, 2012.

[9] C. Daley, S. Alawneh, D. Peters, B. Quinton, and B. Colbourne, "GPU modeling of ship operations in pack ice," in *Proc. Int. Conf. ICETECH Exhib. Perform. Ships Struct.*, Banff, AB, Canada, 2012, pp. 122–127.

[10] G. Vachon, M. Sayed, and I. Kubat, "Methodology for determination of ice management efficiency," in *Proc. Int. Conf. ICETECH Exhib. Perform. Ships Struct.*, Banff, AB, Canada, 2012, pp. 346–353.

[11] M. Sayed *et al.*, "Numerical simulations of ice interaction with a moored structure," in *Proc. Int. Conf. ICETECH Exhib. Perform. Ships Struct.*,
Banff, AB, Canada, 2012, pp. 159–166.

[12] M. Sayed, I. K. Kubat, and B. Wright, "Numerical simulations of ice forces on the Kulluk: The role of ice confinement, ice pressure and ice
management," in *Proc. OTC Arctic Technol. Conf.*, Houston, TX, USA,2012, pp. 965–973.

[13] A. Gürtner, B. Bjørnsen, T. H. Amdahl, S. R. Sberg, and S. H. Teigen, "Numerical simulations of managed ice loads on a moored Arctic drillship,"
in *Proc. OTC Arctic Technol. Conf.*, Houston, TX, USA, 2012, pp. 914–920.

[14] I. Metrikin, S. Løset, N. A. Jenssen, and S. Kerkeni, "Numerical simulation of dynamic positioning in ice," *Marine Technol. Soc. J.*, vol. 47,
no. 2, pp. 14–30, Mar./Apr. 2013.

[15] B. Wright *et al.*, "Evaluation of full scale data for moored vessel stationkeeping in pack ice," B. Wright & Associates Ltd., Canmore, AB, Canada,
PERD/CHC Report 26-200, 1999.

[16] J. Haugen, L. Imsland, S. Løset, and R. Skjetne, "Ice observer system for ice management operations," in *Proc.*

21st Int. Ocean Polar Eng. Conf., Maui, HI, USA, 2011, p. 1120.
[17] P. Lu, Z. Li, Z. Zhang, and X. Dong, "Aerial observations of floe size distribution in the marginal ice zone of summer Prydz Bay,"*J. Geophys. Res., Oceans*, vol. 113, no. C2, pp. C02011-1–C02011-11,
Feb. 2008.
[18] Q. Zhang, R. Skjetne, S. Løset, and A. Marchenko, "Digital image processing for sea ice observation in support to Arctic DP operation," presented at the Proc. 31st International Conf. Ocean, Offshore Arctic Engineering, Rio de Janeiro, Brazil, 2012, Paper OMAE2012-83860.
[19] M. Eldridge *et al.*, "Design and build a search and rescue UAV," Univ. Adelaide, Adelaide, Australia, 2009.
[20] T. Toyota, S. Takatsuji, and M. Nakayama, "Characteristics of sea ice floe size distribution in the seasonal ice zone," *Geophys. Res. Lett.*, vol. 33,
no. 2, pp. L02616-1–L02616-4, Jan. 2006.
[21] T. Toyota, C. Haas, and T. Tamura, "Size distribution and shape properties of relatively small sea-ice floes in the Antarctic marginal ice zone in late winter," *Deep Sea Res. II, Top. Studies Oceanogr.*, vol. 58, no. 9/10, pp. 1182–1193, May 2011.
[22] Q. Zhang, S. van der Werff, I. Metrikin, S. Løset, and R. Skjetne, "Image processing for the analysis of an evolving broken-ice field in model testing," presented at the 31st Int. Conf. Ocean, Offshore Arctic Engineering, Rio de Janeiro, Brazil, 2012, Paper OMAE2012-84117.
[23] J. Blunt, V. Garas, D. Matskevitch, J. Hamilton, and K. Kumaran, "Image analysis techniques for high Arctic, deepwater operation support," in *Proc. OTC Arctic Technol. Conf.*, Houston, TX, USA, 2012, pp. 986–996.
[24] Q. Zhang, R. Skjetne, and B. Su, "Automatic image segmentation for boundary detection of apparently connected sea-ice floes," in *Proc. 22nd*
Int. Conf. Port Ocean Eng. Arctic Conditions, Espoo, Finland, 2013, pp. 303–310.
[25] J. Banfield, "Automated tracking of ice floes: A stochastic approach," *IEEE Trans. Geosci. Remote Sens.*, vol. 29, no. 6, pp. 905–911, Nov. 1991.
[26] J. D. Banfield and A. E. Raftery, "Ice floe identification in satellite images using mathematical morphology and clustering about principal curves,"
J. Amer. Stat. Assoc., vol. 87, no. 417, pp. 7–16, Mar. 1992.
[27] C. Xu and J. L. Prince, "Snakes, shapes, and gradient vector flow," *IEEE Trans. Image Process.*, vol. 7, no. 3, pp. 359–369, Mar. 1998.
[28] N. Otsu, "A threshold selection method from gray-level histograms," *Automatica*, vol. 11, no. 285–296, pp. 23–27, 1975.
[29] J. MacQueen *et al.*, "Some methods for classification and analysis of multivariate observations," in *Proc. 5th Berkeley Symp. Math. Stat. Probab.*, Berkeley, CA, USA, 1967, vol. 1, pp. 281–297.
[30] M. Kass, A. Witkin, and D. Terzopoulos, "Snakes: Active contour models," *Int. J. Comput. Vis.*, vol. 1, no. 4, pp. 321–331, Jan. 1988.
[31] A. Rosenfeld and J. L. Pfaltz, "Distance functions on digital pictures,"
Pattern Recognit., vol. 1, no. 1, pp. 33–61, Jul. 1968.
[32] R. C. Gonzalez, R. E.Woods, and S. L. Eddins, *Digital Image Processing Using MATLAB*. Upper Saddle River, NJ, USA: Prentice-Hall, 2003.
[33] L.-K. Soh, C. Tsatsoulis, and B. Holt, "Identifying ice floes and computing ice floe distributions in SAR images," in *Analysis of SAR Data of the Polar Oceans*. Berlin, Germany: Springer-Verlag, 1998, pp. 9–34.
[34] WMO SEA-ICE NOMENCLATURE, (accessed 2014-08-31). [Online]. Available: http://www.aari.ru/gdsidb/XML/volume1.php?lang1=0& arrange=4
[35] P. Lu and Z. Li, "A method of obtaining ice concentration and floe size from shipboard oblique sea ice images," *IEEE Trans. Geosci. Remote Sens.*, vol. 48, no. 7, pp. 2771–2780, Jul. 2010.
[36] Qin Zhang,Roger skjetne"Image Techniques for Identifying Sea-Ice Parameters" Modelling,Identification and Control,Vol 35,N0.4,2014,pp.293-301 ISSN1890-1328
[37]Mengmeng Zhang,Qianqian li,Lei Li,peirui bai,"An Improved Algorithm based on the GVF-Sanke for Effective Concavity Edge Detection" Journal of Software Engineering and applications,201,6,174-178
[38]S.SriSudha,A.Senthil Kumar,D.S.Jain and V.K.Dadhwal,"Detection and size distribution analysis of ice floes near Antarctica using RISAT-1 imagery"CURRENTSCIENCE,VOL105,No10, 25November2013
[39]Qin Zhang,Solange vander Werff,Ivan Metrikin,Sveinung Laset,Roger Skjetne,"Image Processing for the analysis of an evolving broken-ice field in model testing"in Proc.ASME 2012,31st International Conference on Ocean,Offshore and Arctic Engineering,july 1-6,2012
[40]Takenobu Toyota,Shinya Takatsuji andMasashigeNakayama,"Characteristics of sea ice floessize distribution in the sea ice zone"geo Physical Research letters,vol.33.2006

Author's Profile:

P.Gangadhara Reddy Presently Working as a Assistant Professor in Dept of ECE in Aditya College of Engineering, Madanapalle, India. Received His M.Tech in-LICS From Sri Venkateswara University,Tirupati ,Obtained B.Tech in –ECE From Rajiv Gandhi College of Engineering &Technology,Nandyal.Now He pursuing his Ph.D degree from Sri Venkateswara University,Tirupati.

His Research Areas include Image & Signal Processing and Communication systems.